Effect of ionic strength on the formal potential of the glass electrode in various saline media

Isabel Brandariz[a], Teresa Vilariño[a], Pablo Alonso[a], Roberto Herrero[a], Sarah Fiol[b], Manuel E. Sastre de Vicente[a,]

Talanta,

Volume 46, Issue 6, August 1998, Pages 1469–1477

Received 27 May 1997, Revised 21 October 1997, Accepted 19 December 1997, Available online 4 December 1998

DOI:10.1016/S0039-9140(98)00022-8

Abstract

We examined the variation with ionic strength (*I*, adjusted with KCl, KNO_3, KBr, NaCl or $NaClO_4$) of the formal potential (E_{const}) for glass electrodes exhibiting a Nernstian response (i.e. $E_{cell}=E_{const}-s \log [H^+]$). For this purpose, we investigated the different factors included in the formal potential, so we obtained reported values for the liquid junction potential as a function of ionic strength and determined the logarithm of the activity coefficient for the proton in various saline media, using Pitzer equations.

Keywords

Ionic strength; Formal potential; Glass electrode; Potentiometry

[a] Departamento de Química Fundamental e Industrial, Facultad de Ciencias, Universidad de La Coruña, Campus da Zapateira s/n, E-15701 La Coruña, Spain

[b] Departamento de Química Física, Facultad de Química, Universidad de Santiago de Compostela, E-15706 Santiago de Compostela, Spain

1. Theoretical background

Potentiometry with a commercially available H^+ ion-sensitive glass electrode, also referred to as 'pH-metry', is a powerful tool for determining equilibrium constants [1]. IUPAC recommends calibrating glass electrodes in terms of the proton concentration at a constant ionic strength prior to the determination proper [2]. Glass electrodes exhibit a Nernstian response; consequently, the resulting electromotive force at constant ionic strength will be given by [3]

$$E_{\text{cell}} = E_{\text{const}}(I) + s \log [\text{H}^+] \quad (1)$$

where

$$E_{\text{const}} = E_{\text{r}} + E_{\text{l}} + E_g^a + \text{s} \log \gamma_{\text{H}^+} \quad (2)$$

and *s* denotes the Nernstian slope, the value of which at 25°C is

$$s = \ln 10 \quad RT / F = 59.16 \text{ mV} \quad (3)$$

In Eq. (2), E_g^0 is the potential across the glass membrane at unity proton activity; E_r is the combination of the external and internal reference potentials and will thus be independent of the ionic strength of the unknown solution—unlike the liquid junction potential (E_l) and, obviously, the activity coefficient for the proton ($\log \gamma_{H^+}$). According to the Stockholm school [4], E_l varies with acidity; however, several authors have shown that it can be assumed not to vary, within experimental errors, with small acidity changes (e.g. over the $-\log [H^+]$ ranges 2.3–2.9 and 10.8–11.3). In addition, fulfillment of Eq. (1)has been experimentally confirmed 3 and 5.

Parameter E_g^0 encompasses the asymmetry potential, resulting from differences between the inner and outer leached layers and potentially arising from composition differences introduced during the electrode's manufacturing process, a differential history for both leached layers or the adsorption of given substances by either [6].

Although formal potentials, E_{const}, are commonly used to determine equilibrium constants, virtually none of the studies involving calibration of glass electrodes in terms of the proton concentration 7, 8, 9, 10, 11 and 12has reported on the variation of E_{const} with ionic strength [$E_{\text{const}}=f(I)$]. One interesting exception is the study of Pezza et al. [13], who used various ion-selective electrodes to determine the activity coefficients for the ions sensed by each electrode. In this work, we used commercially available H^+ ion-sensitive glass electrodes to compare the variation of the formal potential with ionic strength in five different electrolytes that are commonly used to adjust the latter parameter (NaCl, KCl, KBr, KNO_3 and $NaClO_4$).

2. Experimental

Calibrations were done in an acid medium[1] as described elsewhere [5]:variable volumes v of a strong acid of concentration c were successively added to an initial volume V_0 of inert electrolyte solution. The proton concentration was thus given by

$$[H^+] = \frac{cv}{V_0 + v} \quad (4)$$

where $2.3 < -\log [H^+] < 2.9$ [3]. We used an initial volume V_0=40.0 ml to which 0.04 ml aliquots of 0.1000 M HCl were successively added. Only those points included in the above-mentioned range were used to fitE_{cell} versus log $[H^+]$ curves.

We carried out experiments at a variable ionic strength adjusted with NaCl, KBr, KNO_3, KCl and $NaClO_4$ (all Merck p.a. reagents). The water used to prepare every solution was purified by passage through a Millipore Milli-Q system. All experiments were performed in a dual-wall cell through which water thermostated at 25.0±0.1°C was circulated. Nitrogen of 99.999% purity was bubbled through the cell to remove CO_2 and stir the solution. A Crison microBU 2030 autoburette furnished with a 2.5 ml syringe for dispensing the titrant was used. The burette was controlled via a computer that afforded reading the emf of a Crison micropH 2002 pH-meter connected to a Radiometer GK2401C electrode. This last was a glass electrode combined with an Ag/AgCl reference electrode where the liquid junction was established by a salt bridge consisting of a plug of porous ceramics.

3. Results and discussion

Fig. 1 shows a typical calibration curve, of intercept E_{const}=378.9±0.1 mV and slope 59.1±0.1 mV. TheE_{const} values obtained from similar fitted curves for the different electrolytes are shown in Fig. 2 Fig. 4 and Fig. 5. By way of example, Fig. 3 shows the slopes of the calibration curves obtained in KNO_3; as can be seen, there were no significant deviations from 59.2 mV at 25°C—the largest error was 2%—,which testifies to the Nernstian behaviour of the electrode. Similar results were obtained regarding the slopes of the fitted curves for the other electrolytes. On the other hand, careful examination of Fig. 2 reveals increased dispersion of formal potentials in graph D. The difference arose from the fact that, except in series 1D, the glass electrode was stored in a slightly acidic solution (about 0.05 M) while not in use in order to improve its response relative to storage in water or a neutral buffer [14]. During the calibrations of Fig. 2D, the electrode was kept in distilled water while not in use—an identical behaviour was observed if it was stored in a neutral buffer.

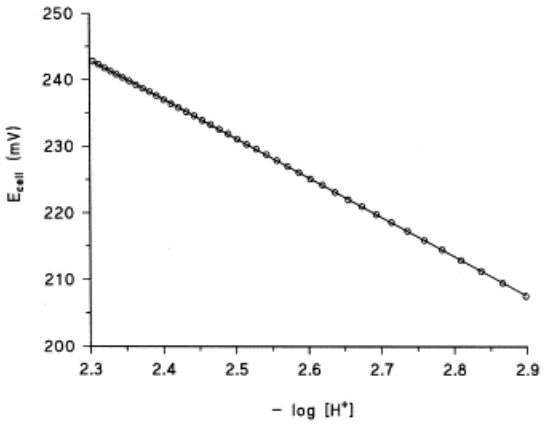

Fig. 1.
Calibration curve of equation E=378.9 (± 0.1)−59.1 (± 0.1) p[H^+] in 0.6 M KBr.

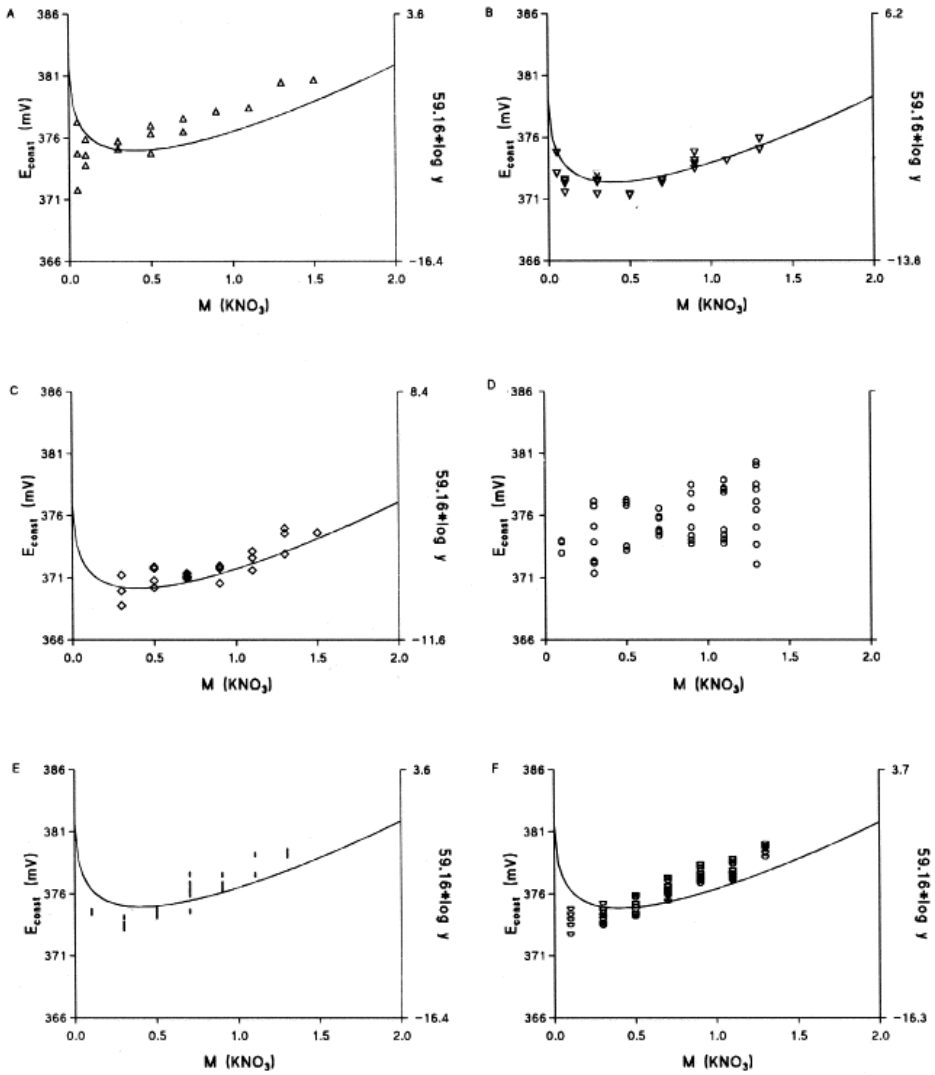

Fig. 2. Variation of E_{const} with I in KNO_3. Data obtained with the same Radiometer GK2401C electrode on the following time frames: (A) May–June, 1992, (B) April, 1993, (C) January–April, 1994, (D) October, 1994, (E) December, 1994, and (F) February–March, 1995. The solid line represents the variation of s log γ_{H^+} with I according to the Pitzer equations.

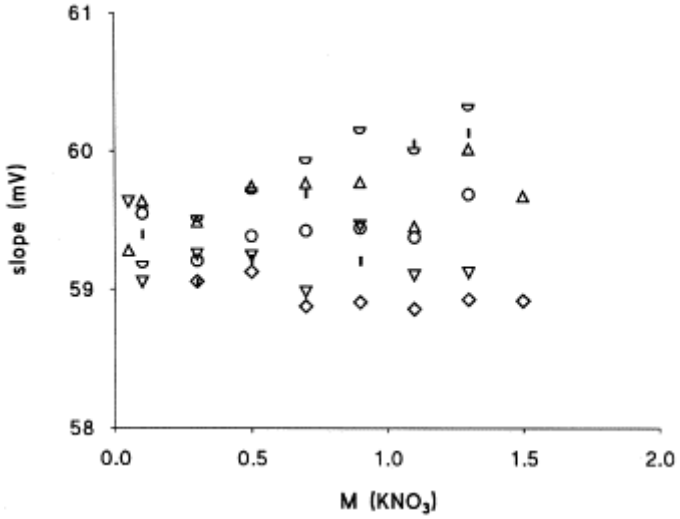

Fig. 3.
Mean of the slopes of the calibration curves in Fig. 2.

As can also be seen from Fig. 2, experimental points in the E_{const} versus I graphs followed the same pattern, albeit shifted to lower or higher potentials—note that the same scale was used in all graphs.

In order to account for the behaviour of these E_{const} versus I curves in Fig. 2 and Fig. 4 Fig. 5 one must break down E_{const} into the factors included in Eq. (2). As noted earlier, both the liquid junction potential, E_l, and the activity coefficient for the proton, vary with ionic strength.

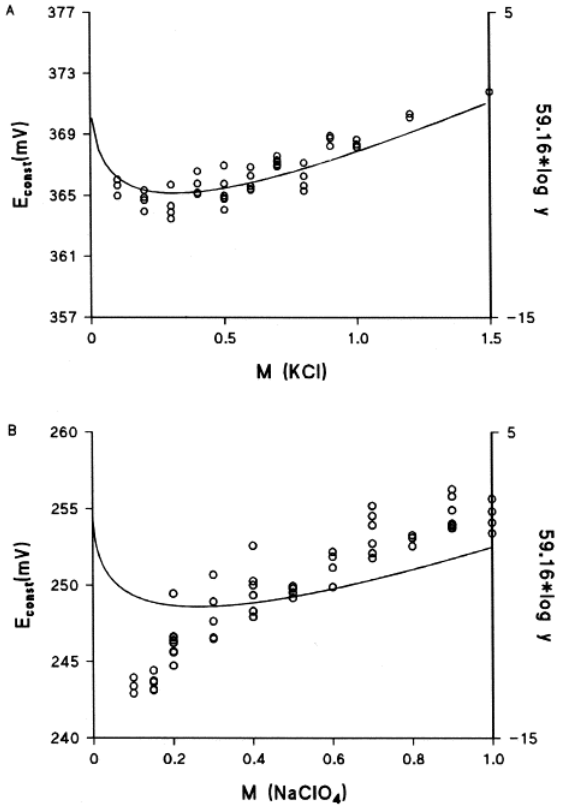

Fig. 4.
Variation of E_{const} with I in the following electrolytes: (A) KCl and (B) $NaClO_4$. The solid line represents the variation of $s \log \gamma_{H^+}$ with I according to the Pitzer equations.

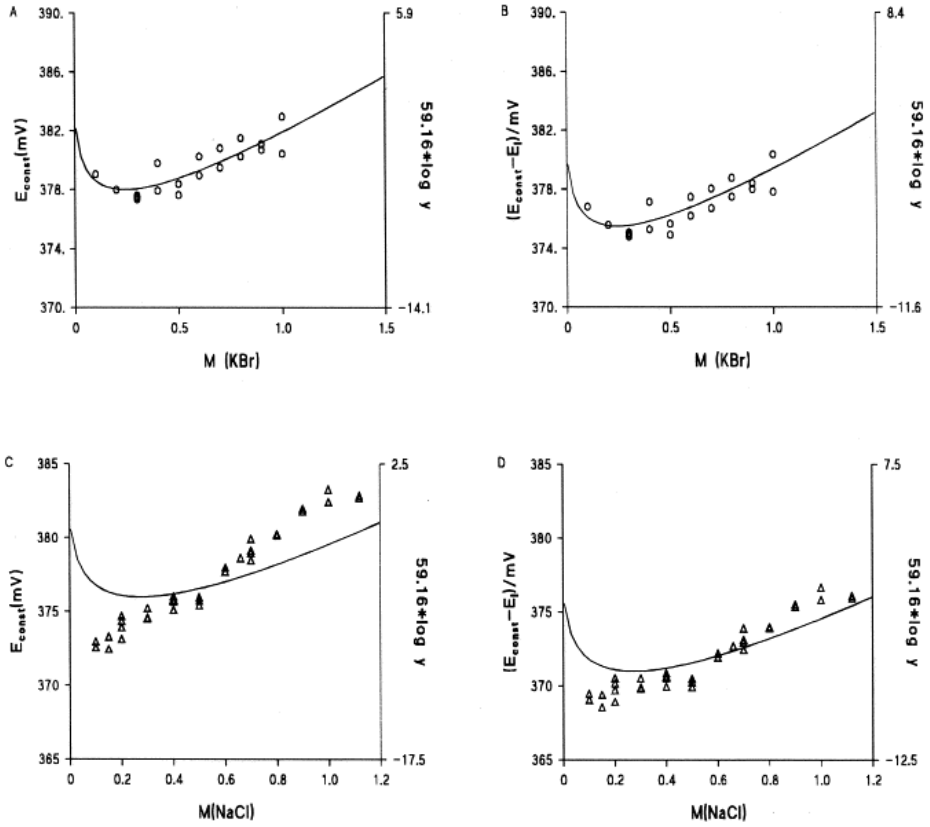

Fig. 5.
Variation of (A) E_{const} with I in KBr, (B) $E_{const}-E_l$ with I in KBr, (C) E_{const} with I in NaCl, and (D) $E_{const}-E_l$ with I in NaCl. The solid line represents the variation of $s \log \gamma_{H^+}$ with I according to the Pitzer equations.

There are few reported liquid junction potentials. By exception, Bagg [15] has reported the potentials for the junction or free diffusion between a 4 M KCl solution and NaCl or KBr solutions at a variable ionic strength (Fig. 6). The results of Bagg [15] for the liquid junction residual potential in dual-junction cells are comparable, within experimental error for this type of measurement, with those experimentally—derived in almost every system studied so far. As noted by Bagg himself, 'this agreement is particularly satisfactory in view of (a) the probable differences of the junctions, sleeve-type and frit, used in the cells from the idealized model of junction used in the calculation, and (b) the extrapolation of some transference numbers beyond the range of concentration in which they are determined.'

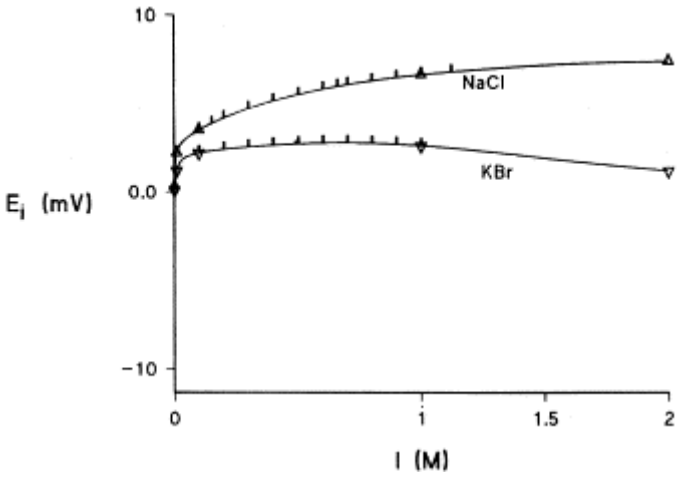

Fig. 6.
Variation of E_l with I in NaCl and KBr. Triangles represent data from an earlier reference [15] and ticks the points where E_l was extrapolated.

The sole constraint to the use of the previous data [15] is that the ionic strength values used do not coincide with those of our experiments, so E_l must be interpolated to the desired I values. For this purpose, we used a polynomial ratio proposed elsewhere [16] as the interpolation function. We used this type of function because it fits the experimental behaviour more closely than does a simple polynomial or a cubic spline interpolation function [16].

Provided the liquid junction potential is known, Eq. (2) can be rewritten as

$$E_{const} - E_l = E_r + E^0_g + s \log \gamma_{H+} \quad (5)$$

If the only term that depends on ionic strength on the right-hand side of this equation is the activity coefficient for the proton, then, the plots of (E_{const}−E_1) versus I and (s log [H^+]) versus I should exhibit the same trend except for the shift due to the $(E_r + E^0_g)$term. In order to confirm this assumption, we superimposed the (s log γ_{H^+}) versus I curve and shifted it to overlap the previous one, obviously, at the same scale amplitude (20 mV) in both cases (Fig. 5B,D).

The activity coefficient for the proton was calculated in the light of Pitzer's formalism. The pertinent equations are given in Appendix Aand the curves obtained in the different electrolytes studied are shown inFig. 7. As can be seen, every curve exhibits a minimum at a different ionic strength for each electrode, beyond which the curve is virtually linear. The similar behaviour of the (s log γ_{H^+}) versus I curves and the (E_{const}−E_l) versus I curves is apparent in Fig. 5B,D for KBr and NaCl, respectively. One quantitative way of comparing the experimental results with the curve derived from the Pitzer equations is by fitting experimentalE_{const} versus I data points and those in the (s log γ_{H^+}) versus I curve obtained from the Pitzer equations—obviously in the virtually linear zone (Fig. 7)—to a straight line. Table 1 gives the results obtained and the ionic strength range used in each fitting. As can be seen, consistency between data is quite good for KBr (Fig. 5B) but not quite for NaCl (Fig. 5D) as the likely result of Na^+ ion influencing the behaviour of the glass electrode. Unfortunately, there seems to be no

reported liquid junction potentials for the other systems studied, so we chose to plot E_{const} versus I and (s log γ_{H}^{+}) versus I in the same graphs.

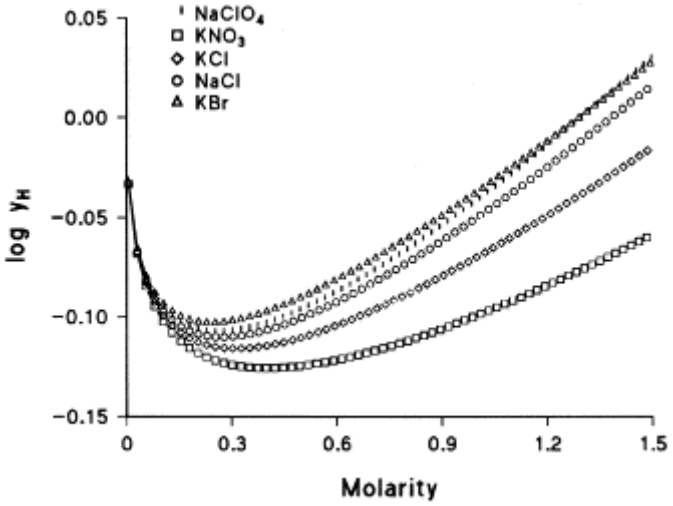

Fig. 7.
Variation of log γ_{H}^{+} with I (on the molar scale) in $NaClO_4$, KNO_3, KCl, NaCl and KBr.

Table 1.: Slopes of the linear fits of E_{const} versus I, (E_{const}−E_l) versus I and slog γ_{H}^{+}versus I plots in each of the electrolytes studied

Electrolyte	59.16×log y [a] (Pitzer eq.)	Slope of E_{const} vs. I	Slope of E_{const}−E_l vs. I	I range	Fig.
KNO_3	4.0±0.1	4.8±0.7		0.5–1.5	2a
	4.0±0.1	5.1±0.6		0.5–1.5	2b
	4.0±0.1	3.7±0.6		0.5–1.5	2c
	4.0±0.1	5.7±0.8		0.5–1.5	2e
	4.0±0.1	5.0±0.3		0.5–1.5	2f
KCl	6.2±0.1	6.7±0.6		0.5–1.5	4a
$NaClO_4$	6.5±0.1	9.9±1.4		0.5–1.0	4b
KBr	6.3±0.1	6.6±1.5	6.8±1.4	0.5–1.0	5a,b
NaCl	6.0±0.1	11.4±0.5	9.0±0.5	0.4–1.1	5c,d

a Obtained from those points in Fig. 7 that lay within the stated ionic strength range for each electrolyte.

As can be seen from both Table 1 and Fig. 5A, the results in KBr were still similar, which was to be expected since E_l remained virtually constant throughout the ionic strength range studied. Similar consistency was observed in KCl and KNO_3 (Table 1, Fig. 2 and Fig. 4A), which suggests that E_l remains virtually constant over the ionic strength range where the formal potential was determined. Fig. 2 also shows six data series for the formal potential; while all exhibit a similar trend, the potential is displaced to a greater or lesser extent between one another. Based on Eq. (5), this can be ascribed to change in the $(E_r + E_g^0)$ term because, if the electrodes were theoretically immersed in the same solutions, E_r should have remained constant and the change be due to a variation in the asymmetry potential with time typical of changes at the electrode surface layer.

The E_{const} versus I plot in sodium perchlorate exhibited a much greater slope than that obtained from the Pitzer fitting as the likely result of (a) the influence of sodium ion on glass membranes and/or (b) a major change in the liquid junction potential relative to potassium salts over the ionic strength range studied.

Appendix A.

The relationship of $\log \gamma_{H^+}$ to I was studied in the light of the Pitzer equations [17], which have frequently been used to describe the influence of ionic strength on the activity coefficients for strong electrolytes at moderate to high concentrations and a high electrolyte concentration. Our group has used them to interpret the variation with ionic strength of the acidity constants for some organic molecules 18, 19, 20, 21, 22, 23,24, 25 and 26.

Based on Pitzer's formalism, the activity coefficient for H^+ ion in the presence of excess electrolyte is given by

$$\ln \gamma_{H+} = f^{\gamma} + 2I(B_{XH} + IC_{XH}) + I^2(B'_{XK} + C_{XK}) + I(2\theta_{HK} + I\psi_{HXK}) \quad (A.1)$$

where the ionic strength is determined from the salt concentration since the salt is in a large excess relative to the proton. f', B and B' depend on I, as can be seen in the following equations:

$$f^{\gamma} = -A_{\phi}\left[\frac{\sqrt{I}}{1+1.2\sqrt{I}} + \frac{2}{1.2}\ln\left(1+1.2\sqrt{I}\right)\right] \quad (A.2)$$

$$B_{XK} = \beta^{(0)}_{XK} + \frac{\beta^{(1)}_{XK}}{2I}\left[1 - \left(1+1.2\sqrt{I}\right)\exp\left(-2\sqrt{I}\right)\right] \quad (A.3)$$

$$\beta'_{XK} = \beta^{(0)}_{XK} + \frac{\beta^{(1)}_{XK}}{2I}\left[-1 + \left(1 + 1.2\sqrt{I} + 2I\right)\exp\left(-2\sqrt{I}\right)\right] \quad \text{(A.4)}$$

Substituting B and B' in the expression for the logarithm of the activity coefficient of H^+ ion yields

$$\ln \gamma_{H+} = f^{\gamma} + PI + QI^2 + RI\,e^{-2\sqrt{I}} + T\left[1 - \left(1 + 1.2\sqrt{I}\right)e^{-2\sqrt{I}}\right] \quad \text{(A.5)}$$

where

$$P = 2\left(\beta^{(0)}_{HX} + \theta_{HK}\right)$$

$$Q = C^{\phi}_{HX} + \frac{C^{\phi}_{KX}}{2} + \psi_{HXK}$$

$$R = \beta^{(1)}_{KX}$$

$$T = \beta^{(1)}_{HX} - \frac{\beta^{(1)}_{KX}}{2} \quad \text{(A.6)}$$

P, Q, R and T are thus constants that depend on the particular inert electrolyte (see Table 2). The Pitzer parameters used to calculate them were taken from an earlier reference [17].

Table 2. Pitzer Parameters used in Eq. (A.5)for each of the electrolytes studied

Electrolyte	*P*	*Q*	*R*	*T*
KNO_3	0.2338	0.0043	0.0494	0.2959
KCl	0.3650	−0.0062	0.2122	0.1884
KBr	0.4020	−0.01363	0.2212	0.2458
NaCl	0.4270	−0.0026	0.2664	0.1613
$NaClO_4$	0.4214	−0.00899	0.2755	0.15535

The activity coefficients in Eq. (A.5)are expressed on the molal scale, so they must be converted into molar units since E_{const} was determined from molar [H^+] values. We used the following equation for this purpose[27]:

$$y = \gamma \frac{\rho_w}{\rho} \left(1 + \sum_i m_i . M_i\right) \quad \text{(A.7)}$$

where y and γ denote the activity coefficients on the molar and molal scale, respectively; ρ is the solution density; ρ_w is water density at the working temperature; i denotes any ion in solution; and Mi is the molar mass of ion i, mi is molality and ci its molarity.

By way of example, substituting water density at 25°C and the molecular mass of NaCl into Eq. (A.7) yields

$$y_{NaCl} = \frac{\gamma_{NaCl}}{\rho_{NaCl}} (0.997075 + 0.05827\, m_{NaCl}) \quad \text{(A.8)}$$

Also, molality can be converted into molarity by using the following expression:

$$\frac{c}{m} = \frac{\rho_{NaCl}}{1 + \sum_i m_i . M_i} \quad \text{(A.9)}$$

which, for NaCl, becomes

$$c_{NaCl} = \frac{\rho_{NaCl}\, m_{NaCl}}{1 + 0.10110 m_{NaCl}} \quad \text{(A.10)}$$

The dependence of density on the ionic strength can be determined by fitting ρ versus m data pairs to a polynomial expression of m based on reported values 28 and 29.

References

1. E.P. Serjeant

   Potentiometry and Potentiometric TitrationsWiley, New York (1984)

2. A. Braibanti, G. Ostaroli, P. Paoleti, D. Petit, S. Sammartano

   Pure Appl. Chem., 59 (12) (1987), p. 1721

3. P.M. May, D.R Williams, P.W. Linder, R.G. Torrington

   Talanta, 29 (1982), p. 249

4. P.W. Linder, R.G. Torrington, D.R. Williams

   Analysis using Glass Electrodes, Ch. 4Open University Press, Oxford (1984)

5. S. Fiol, F. Arce, X.L. Armesto, F. Penedo, M. Sastre de Vicente

   Fresenius J. Anal. Chem., 343 (1992), p. 469

6. H. Galster

   pH MeasurementVCH, New York (1991)

7. W.A.E. Mcbryde, Analyst, 96 (1971) p. 739; 94 (1969) p. 337.
8. H.S. Dunsmore, D. Midley

   Anal. Chim. Acta, 61 (1972), p. 115

9. M.T.S.D. Vasconcelos, A.S.C. Machado

   Rev. Port. Quim., 28 (1986), p. 120

10. E.W. Baumann

    Anal. Chim. Acta, 64 (1973), p. 284

11. H.M. Irving, M.G. Miles, L.D. Petit

    Anal. Chim. Acta, 38 (1967), p. 475

12. G.R. Hedwig, H.K.J. Powell

    Anal. Chem., 43 (10) (1971), p. 1206

13. L. Pezza, M. Molina, M. de Moraes, C.B. Melios, J.O. Tognolli

    Talanta, 43 (1996), p. 1689

14. W.H. Beck, J. Caudle, A.K. Covington, W.F.K. Wynne-Jones, Proc. Chem. Soc., (1963) 110.
15. J. Bagg

    Electrochim. Acta, 35 (2) (1990), pp. 361–367

16. W.H. Press, S.A. Teukolsky, W.T. Veterling, B.P. Flannery

    Numerical Recipes in Fortran Ch., 3 (2nd ed.)Cambridge University Press, Cambridge (1992)

17. K.S. Pitzer

    Theory: ion interaction approach

    K.S. Pitzer (Ed.), Activity Coefficients in Electrolyte Solutions. (2), CRC Press, Boca Ratón, Fl (1991), p. 75

18. R. Herrero, X.L. Armesto, F. Arce, M. Sastre de Vicente

    J. Solution Chem., 21 (11) (1992), p. 1185

19. I. Brandariz, F. Arce, X.L. Armesto, F.J. Penedo, M. Sastre de Vicente

    Monatsh. Chem., 124 (1993), p. 249

20. R. Herrero, I. Brandariz, M. Sastre de Vicente

Ber. Bunsenges. Phys. Chem., 97 (1) (1993), p. 59

21. I. Brandariz, R. Herrero, M. Sastre de Vicente

    J. Chim. Phys., 90 (1993), p. 63

22. H. Herrero, I. Brandariz, S. Fiol, M. Sastre de Vicente

    Collect. Czech. Chem. Commun., 58 (1993), p. 1269

23. S. Fiol, I. Brandariz, X.L. Armesto, F. Arce, M. Sastre de Vicente

    Ann. Chim. (Rome), 83 (1993), p. 175

24. I. Brandariz, S. Fiol, R. Herrero, T. Vilariño, M. Sastre de Vicente

    J. Chem. Eng. Data, 38 (1993), p. 531

25. S. Fiol, I. Brandariz, R. Herrero, T. Vilariño, M. Sastre de Vicente

    Ber. Bunsenges. Phys. Chem., 98 (1994), p. 164

26. R. Herrero, I. Brandariz, S. Fiol, T. Vilariño, M. Sastre de Vicente

    An. Quím., 89 (5) (1993), p. 602

27. F. Macintyre

    Mar.Chem., 4 (1970), p. 205

28. R.C. Weast (ed.), C.R.C. Handbook of Chemistry and Physics, C.R.C. Press, Boca Raton, Florida, 1986,

29. J.F. Chem, G.R. Choppin

    J. Solution Chem., 24 (5) (1995), p. 46

Corresponding author. Tel.:+34 81 167050; fax:+34 81 167065; e-mail: eman@udc.es

If calibration was performed by adding a base to an acid solution, then the combination of relatively small errors in the concentration of both resulted in the slope of the fitted curve deviating from the Nernstian value, as previously noted elsewhere 3 and 5.